Science of the Total Environment 908 (2024) 168411

Contents lists available at ScienceDirect

Science of the Total Environment

journal homepage: www.elsevier.com/locate/scitotenv

Water sources for street trees in mesic urban environments

Ian A. Smith [a,*], Pamela H. Templer [b], Lucy R. Hutyra [a]

[a] Boston University, Department of Earth & Environment, 685 Commonwealth Ave., Boston, MA 02215, USA
[b] Boston University, Department of Biology, 5 Cummington Mall, Boston, MA 02215, USA

HIGHLIGHTS

- Water source utilization and partitioning in street trees is data limited.
- We used natural abundance stable isotopes to estimate proportional sources of water.
- Precipitation was the dominant source of street tree water uptake.
- Tree cover correlated with the amount of precipitation lost to evapotranspiration.
- Precipitation dependency may lead to increased water stress in a changing climate.

GRAPHICAL ABSTRACT

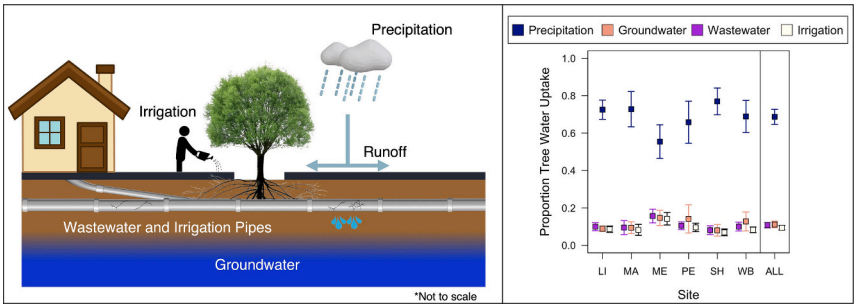

ARTICLE INFO

Editor: Jurgen Mahlknecht

Keywords:
Urban greening
Stable isotopes
Precipitation
Irrigation
Evapotranspiration
Ecosystem services

ABSTRACT

Street trees support climate resiliency through a variety of pathways, such as offsetting urban heat and attenuating storm water runoff. While urban trees in arid and semiarid ecosystems have been shown to take up water from irrigation, it is unknown where street trees in mesic cities obtain their water. In this study, we use natural abundance stable isotopes to estimate the proportional sources of water taken up by *Acer platanoides* street trees in Boston, Massachusetts, United States, including precipitation, irrigation, groundwater, and wastewater. We use Bayesian multisource mixing models to estimate water sources by comparing the natural abundance isotopic ratios of hydrogen and oxygen across potential water sources with water extracted from tree stem samples. We find that during the summer of 2021, characterized by anomalously high rainfall, street trees predominantly utilized water from precipitation. Precipitation accounted for 72.3 % of water extracted from trees sampled in August and 65.6 % from trees sampled in September. Of the precipitation taken up by street trees, most water was traced back to large storm events in July, with July rainfall alone accounting for up to 84.0 % of water found within street trees. We find strong relationships between canopy cover fractions and the proportion of precipitation lost to evapotranspiration across the study domain, supporting the conclusion that tree planting initiatives result in storm water mitigation benefits due to utilization of water from precipitation by urban vegetation. However, while the mature trees studied here currently support their water demand from precipitation, the dependency of street trees on precipitation in mesic cities may lead to increased water stress in a changing climate characterized by a higher frequency and severity of drought.

* Corresponding author.
E-mail address: iasmith@bu.edu (I.A. Smith).

https://doi.org/10.1016/j.scitotenv.2023.168411
Received 12 July 2023; Received in revised form 20 October 2023; Accepted 5 November 2023
Available online 7 November 2023

1. Introduction

The majority of the global population currently lives in cities with the world's urban population forecast to reach 6.7 billion by 2060 (United Nations Department of Economic and Social Affairs Population Division, 2018). Hazardous urbanization-induced environmental conditions experienced by urban dwellers such as increased heat exposure (Oke, 1982), degraded air quality (Fenger, 1999), and heightened flood risk (Jha et al., 2012) can decrease human health (Galea and Vlahov, 2005) and deteriorate public quality of life and well-being (Krefis et al., 2018). In response, cities are working to identify localized solutions that alleviate the environmental impacts of urbanization, with tree planting initiatives emerging as a promising nature-based strategy with widespread global adoption (Food and Agriculture Organization of the United Nations, 2018).

Trees in cities provide a myriad of services to urban populations, including climate regulation (Bowler et al., 2010), flood risk reduction (Yao et al., 2015), physical and mental health enhancements (Duncan et al., 2014; South et al., 2018), and potential removal of airborne pollutants (Eisenman et al., 2019). Street trees, defined here as trees managed by networks of multi-stakeholder governance located in public right-of-way's that are commonly confined to tree pits and planters, are a primary component of tree planting initiatives. However, street trees are characterized by high mortality rates, especially among newly planted saplings and large, mature trees (Smith et al., 2019), pointing to the need for improved understanding of street tree management, maintenance, and resource acquisition as a necessary step in realizing the ecosystem service benefits associated with tree planting initiatives. A key limiting factor in urban tree establishment, health, and survival is access to water (Konijnendijk, 2010; Moser et al., 2016). However, our knowledge of urban water source utilization and partitioning in street trees is very data limited.

Urbanization alters the movement of water as it is added, removed, diverted, pumped, and piped to meet economic and population demand (Oke et al., 2017). The relatively high impervious surface fraction of cities increases surface runoff (Shuster et al., 2005), potentially inhibiting street tree root access to infiltrated precipitation. Irrigation is often implemented in arid and semiarid cities to supplement street tree water availability (Gleick et al., 2003) with the trade-off of increased use of potentially scarce water resources. Mesic cities, often without dedicated irrigation protocols for mature vegetation, may encourage watering from residents and stakeholders (e.g. City of Boston, 2021). However, residential irrigation of public street trees is largely focused on saplings. While some trees in natural ecosystems and urban greenspaces have been found to utilize groundwater sources (Marx et al., 2022; Balugani et al., 2017; Bijoor et al., 2012; Miller et al., 2010), street tree access to groundwater may be obstructed by compacted soils and restricted soil volumes in tree pits (Mullaney et al., 2015). Anthropogenically introduced water sources from belowground water and sewer pipes represent additional water sources to street trees via leakage into the soil (Peche et al., 2017) or root infiltration into pipes (Randrup et al., 2001). Understanding which of the many potential water sources that street trees utilize has important implications for street tree management and water conservation.

For example, if street trees primarily access soil water from precipitation, they may be sustained by the precipitation frequency of the current climate, but may become more susceptible to the negative effects of a projected future with increases in the frequency and severity of drought (Seneviratne et al., 2012). In contrast, if street trees are found to utilize water from belowground pipes or groundwater, they may be expected to demonstrate heightened drought resilience at the cost of the integrity of belowground infrastructure or stability of the water table. If street trees rely on irrigation to meet water demand, cities must consider the costs and benefits of street tree health versus water conservation.

Tree water source partitioning is commonly quantified by leveraging variability in the natural abundance stable (non-radioactive) isotope composition of water (expressed as the variation in isotope ratios of oxygen and hydrogen in samples relative to a standard; $\delta^{18}O$ and $\delta^{2}H$) originating from different sources (Ehleringer and Dawson, 1992; Dawson et al., 2002). Isotopes are variants of the same chemical element with an equivalent number of protons (i.e. atomic number) but different number of neutrons, resulting in a different atomic mass. Isotopic fractionation, or the relative partitioning of the heavier and lighter isotopes between two coexisting phases, occurs during phase changes such as evaporation and condensation (Dansgaard, 1964; Allison et al., 1983), leading to unique isotopic composition of water across sources. While there is evidence of isotopic fractionation during root uptake in some plant species, such as halophytes and xerophytes (Ellsworth and Williams, 2007; Vargas et al., 2017), other work finds no change in the ratio of heavy to light isotopes during root uptake by vegetation (Wershaw et al., 1970; Dawson and Ehleringer, 1993; Amin et al., 2021), prompting many studies of tree water source partitioning to assume zero fractionation during root uptake. Thus, it is possible to identify and partition tree water source utilization by quantifying the naturally abundant stable isotopic composition of water within suberized tree stems (Dawson and Ehleringer, 1993), given distinct isotopic signatures across potential water sources with the use of Bayesian stable isotope mixing models (Parnell et al., 2013). Despite decades of research on tree water source identification and a recent exponential increase in the number of studies utilizing stable isotope methodologies (Phillips et al., 2014), urban tree source water partitioning remains vastly understudied (Bijoor et al., 2012; Gómez-Navarro et al., 2019; Marx et al., 2022) and has primarily focused on vegetation within arid and semiarid cities, where irrigation is administered regularly (Bijoor et al., 2012; Gómez-Navarro et al., 2019).

In Los Angeles, California, United States, Bijoor et al. (2012) evaluated the isotopic ratios of urban tree stem water, and potential sources of water for trees, including soil water, irrigation water, and groundwater, finding that the soil water taken up by trees was primarily composed of water originating from irrigation rather than precipitation. In some cases, despite frequent irrigation, some trees accessed groundwater to supplement their water demand. Furthermore, the isotopic composition of stem water in some trees could not be explained by the isotopic composition of irrigation water or groundwater, which Bijoor et al. (2012) speculated may be due to trees utilizing water from runoff, storm drains, or leaky pipes. In Salt Lake City, Utah, United States, Gómez-Navarro et al. (2019) observed variability in tree water source partitioning within urban parks across the growing season, finding water from irrigation to be a dominant source of water within tree stems throughout the growing season, with increasing contributions from snowmelt from the preceding winter towards the end of summer. Marx et al. (2022) assessed ecohydrological partitioning within urban green spaces in Berlin, Germany concluding that while grasses most likely used shallow, younger soil water, urban trees were more dependent on older, deeper soil and groundwater sources.

Here, we conduct, to our knowledge, the first study quantifying urban tree water source partitioning with an explicit focus on street trees in a mesic city that does not provide municipal irrigation of mature trees. We collected water samples from the potential sources, including precipitation, irrigation, groundwater, and wastewater and compared the isotopic ratios to water extracted from suberized street tree stems. We used a Bayesian mixing model analysis to estimate the proportion of water taken up by trees from each source. Mixing model outputs were used to estimate the proportion of precipitation lost to evapotranspiration (ET) to contextualize the implications of street tree water source partitioning on urban water cycling. We tested the hypothesis that street trees in tree pits located in mesic environments primarily rely on precipitation for their water needs. The results provide critical information for the implementation of tree care and planting initiatives for the world's cities in a changing climate.

2. Methods

2.1. Study domain, weather monitoring, and field plots

This study was conducted between May and September 2021 in Boston, Massachusetts, United States. Boston is characterized by a continental, humid climate with warm summers and abundant precipitation. From 1991 to 2020, Boston had a mean annual precipitation rate of 1107 mm yr^{-1}, with an average of 264 mm during the summer months of June, July, and August (JJA; National Centers for Environmental Information, 2023a). The 1991 to 2020 mean annual air temperature was 11.1 °C with a mean JJA air temperature of 22.0 °C (National Center for Environmental Information, 2023a). Precipitation, air temperature, and relative humidity were measured during the study period using a weather station located on the campus of Boston University (Fig. 1).

Six field plots were established within the City of Boston for groundwater and tree sampling (Fig. 1 inset). Each field plot spanned one city block and included a groundwater observation well and five, six, or seven street trees selected for sampling, with a total sample size of $N = 36$ trees across all six plots (Table 1). To reduce variability in water source partitioning estimates due to species-related differences, we restricted our tree sampling to a single species. We chose *Acer platanoides* (Norway maple) as it is the second most abundant street tree species in Boston, making up 9.4 % of the total street tree population and up to 30.5 % of the population at the neighborhood scale, and is uniformly distributed. Norway maple is characterized as one of the ten most abundant species in 14 of 16 neighborhoods described in Boston's Urban Forest Plan (City of Boston, 2022a). All sample trees were mature street trees confined to tree pits, where the City of Boston recommends planting trees in pits such that the sides and bottom of tree pits are open to the surrounding subgrade to allow for root penetration beyond the pit (City of Boston, 2013). Sample trees ranged from 16.0 to 48.5 cm in diameter at breast height (DBH), with an average DBH of 32.8 cm.

2.2. Water and street tree sample collection

Precipitation samples were collected for a subset of rain events during 2021 on the rooftop of the College of Arts and Sciences at Boston University (Fig. 1). Rainwater was collected by funneling water into glass scintillation vials. Once filled, the scintillation vials were immediately capped, sealed, and stored frozen until analysis. Eight precipitation samples were collected for water source partitioning analysis on June 1, June 13, July 2, July 9, August 4, August 8, September 2, and September 10, 2021. Two additional precipitation samples were collected on May 10 and September 28, 2021 to further constrain estimates of the slope and intercept of the local meteoric water line (LMWL), defining the "site-specific covariation of hydrogen and oxygen stable isotope ratios" (Putman et al., 2019), but were not used in the water source partitioning analysis.

Irrigation, wastewater, and groundwater samples were collected on May 16, June 1, July 15, August 10, and September 14, 2021. Irrigation water was sampled from a faucet in the College of Arts and Sciences at Boston University (Fig. 1). The City of Boston primarily receives water from a single source (the Quabbin Reservoir), approximately 110 km west of Boston. Therefore, we use tap water as a reasonable proxy for water used to irrigate street trees, as in Gómez-Navarro et al. (2019). Wastewater grab samples were collected at a local wastewater treatment plant (Fig. 1) from sewage influent. Groundwater samples were collected at each field plot from groundwater wells located on the same city block as sample trees. Prior to sample collection, three times the standing water volume of the well was purged to reduce the influence of evaporatively enriched standing water in the well. Irrigation, wastewater, and groundwater samples were immediately capped, sealed, and stored frozen until analysis. Soil water sampling from tree pits was not feasible due to obstructed soils from impervious tree pit covers (e.g. bricks and pavers) and high root density within tree pits.

Woody, suberized tree stem samples were collected for all 36 trees using a pole pruner from sunlit canopy branches on May 16, June 1, July 15, August 10, and September 14, 2021 between 09:00 and 15:00. Stem samples were approximately 4–6 cm long and approximately 4–10 mm

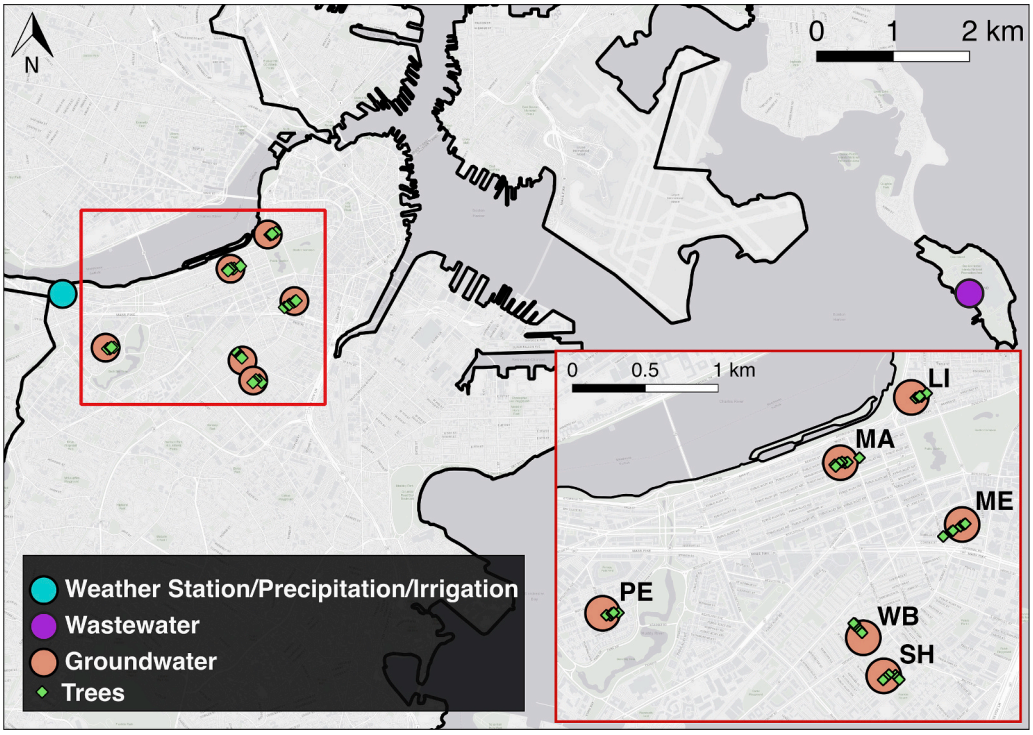

Fig. 1. Main: Location of weather station, sample collection locations, and sample trees. Inset: Six field plots for groundwater and tree sampling labeled by plot ID.

Table 1
Description of field plot characteristics including street name, number of sampled trees, mean diameter at breast height (DBH; cm) of sampled trees, mean impervious surface area (ISA; %) within a 10-meter radius of sampled tree pits (provided at 1-meter resolution by MassGIS, 2005), and a representative example image of a typical sampled tree (© Google Street View).

Plot ID	Street name	# of sampled trees	Mean DBH (cm)	Mean ISA (%)	Image
LI	Lime St.	5	24.5	100	
MA	Marlborough St.	7	35.7	78.7	
ME	Melrose St.	6	35.9	100	
PE	Peterborough St.	6	36.5	83.9	
SH	Shawmut Ave.	6	26.0	66.6	
WB	West Brookline St.	6	38.8	97.8	

in diameter. Stem samples were immediately placed into glass scintillation vials which were capped, sealed, and placed into a cooler with ice until they could be transported to Boston University where they were stored frozen until water extraction. Due to sample loss from inconsistent performance of the isotope ratio mass spectrometers used for analysis of stem samples collected in May, June, and July 2021, only stem samples collected in August and September are included in this analysis. After repair, we confirmed the performance of the isotope ratio mass spectrometer by regular, repeated comparisons with a variety of water standards. Water standards included International Atomic Energy Agency (IAEA)-OH-14 (well water from the great artesian basin in Australia), IAEA-OH-15 (from the Nubian Sandstone Aquifer), IAEA-OH-16 (melted alpine snow from the Austrian Alps), and Vienna Standard Mean Ocean Water (VSMOW) 2 (from three selected fresh water sample from Lake Bracciano, Italy, Lake Galilea, Israel, and a well near Cairo Egypt).

2.3. Proximity of trees to sewer lines and groundwater

The distance of sampled trees to sewer lines and local groundwater depth were determined to assess the feasibility of tree root intrusion. Locations of the primary sewer lines within the six field plots were provided by the Metropolitan Area Planning Council (2021). The sewer line geospatial data does not include all residential connection lines to buildings, resulting in potential overestimates of minimum tree distances to sewer lines. For each tree, the minimum distance from the tree bole to a sewer line was calculated using QGIS version 3.30. Groundwater elevation during the sampling period was provided by the Boston Groundwater Trust (2021). For each field plot, the groundwater depth of the corresponding groundwater observation well was calculated as the difference between the well rim elevation (located at the ground surface in all cases) and groundwater elevation, where elevations were referenced to the Boston City Base Datum (1.72 m).

2.4. Laboratory sample processing

Water from tree stem samples was extracted using cryogenic vacuum distillation at the Boston University Stable Isotope Laboratory, following the methods described in Harrison et al. (2020). Water source and stem water samples were analyzed for stable isotopic composition using an isotope ratio mass spectrometer (GV Instruments IsoPrime) coupled with a Pyr-OH liquid autosampler (Eurovector) at the Boston University Stable Isotope Laboratory. Isotope ratios of hydrogen and oxygen were acquired and expressed in standard delta notation (δ^2H and δ^{18}O; ‰) referenced to the VSMOW standard. Three replicates were run for all precipitation, groundwater, wastewater, and irrigation samples, and two replicates were run for each stem water sample when possible. A total of 36 trees were sampled in both August and September, however, due to a deficiency of water extracted from some samples, we only analyzed 27 trees for August and 31 trees for September 2021. Regular repeated comparisons with several water standards (described above in Methods subsection Water and street tree sample collection) yielded a precision of ±1.85 ‰ for ^{2}H and ±0.25 ‰ for ^{18}O during analysis.

Line-conditioned excess (LC_{xs}; Landwehr and Coplen, 2004) was calculated for each sample to characterize the deviation of the sample isotopic composition from the LMWL due to evaporative enrichment (Birkel et al., 2018). LC_{xs} was calculated as:

$$LC_{xs} = \delta D - a \times \delta^{18}O - b \quad (1)$$

where a is the slope of the LMWL and b is the intercept of the LMWL. More negative LC_{xs} values indicate a higher degree of evaporative enrichment.

2.5. Evapotranspiration modeling

We modeled ET from local vegetation during 2021 to estimate the fraction of precipitation lost to the atmosphere via ET to contextualize the implications of our study results for urban tree storm water mitigation and water availability in a future climate. ET was modeled using the Urban Vegetation Photosynthesis and Respiration Model Latent Heat module, described in detail in Smith et al. (2021), which produces hourly, 30-meter spatial resolution estimates of urban ET based on vegetation activity, urban climate effects, and physiological characteristics. The model was run over six domains corresponding to the six field plots, where domains were created by applying a rectangular buffer of 150 m from each field plot boundary. The proportion of precipitation lost to ET was calculated as the product of mean annual ET (mm) within the modeling domain and the estimated proportion of water uptake from precipitation, divided by the annual precipitation (mm). We estimated relationships between canopy cover and ET across model domains using a linear regression model where canopy cover (%) within each model domain was calculated as the area of tree canopy cover (from a high-resolution land cover product for the City of Boston; University of Vermont Spatial Analysis Laboratory, 2020) divided by the model domain area, multiplied by 100.

2.6. Statistical analysis

Tree stem sample isotope ratios commonly plot below the LMWL

along linear evaporation lines originating from a water source mixture, where the slope of the evaporation lines is a function of temperature, humidity, and equilibrium and kinetic fractionation factors (Benettin et al., 2018). Tree source water isotope ratio mixture distributions were reconstructed from measured isotope ratios using the package 'isoWater' in R (Version 4.1; Bowen, 2022) to account and correct for the effects of source water evaporation during soil infiltration and prior to root uptake. Evaporation line slopes are typically <3 for upper soil layers (Gibson et al., 2008), with flatter slopes under arid conditions (Benettin et al., 2018). We estimated slope priors of 2.58 ($\sigma = 0.17$) and 2.63 ($\sigma = 0.17$) for the August and September 2021 stem sampling dates, respectively, based on eqs. 2–4 and 7 in Benettin et al. (2018), a mean temperature of 22.2 °C, and mean relative humidity of 74 % between June 1 and August 10, 2021 and mean temperature of 22.5 °C and mean relative humidity of 74 % between June 1 and September 14, as measured at the weather station we sampled from (Fig. 1). As the potential street tree water source samples included in the analysis fell on the LMWL, we did not apply evaporation line corrections to precipitation, irrigation, groundwater, or wastewater data.

Using the reconstructed source water mixture found in tree stem samples, we utilized a Bayesian stable isotope multisource mixing model to quantify contributions from each water source to water found within the tree stem for each sampling date using the package 'simmr' in R (Parnell, 2021). The Bayesian framework implements commonly used endmember mixing models, but accounts for uncertainty in isotope composition estimates in tree stem and source samples, utilizes both δ^2H and $\delta^{18}O$ measurements, and provides estimates of water uptake from each source, resulting in a more robust estimate of water source partitioning than other analytical techniques (Rothfuss and Javaux, 2016). This analysis combines Markov chain Monte Carlo (MCMC) sampling with Bayesian updating of prior distributions to estimate a posterior proportion and probability distribution of potential source water contribution to water extracted from tree stems in August and September. For stems collected in August, model inputs of possible water sources include the means and standard deviations of δ^2H and $\delta^{18}O$ estimated from precipitation samples collected in June, July, and August, irrigation sampled in August, wastewater sampled in August, and groundwater sampled in August from the well closest to each tree stem sample. For stems collected in September, model inputs of potential water sources include the means and standard deviations of δ^2H and $\delta^{18}O$ estimated from precipitation samples collected in July, August, and September, irrigation sampled in September, wastewater sampled in September, and groundwater sampled in September from the well closest to each tree stem sample. We chose to use the precipitation samples collected from the same month of tree sampling and two months prior to tree sampling in the analysis since the mean transit time of upper urban soil layers has been estimated to range between 0.64 and 12.11 weeks in tree-covered urban soils (Marx et al., 2022). Including multiple months of precipitation data allows the model to account for tree uptake of soil water that may be composed of a mixture of recent rain events. For each tree stem sampling date, the Bayesian mixing model was run with three chains, 50,000 iterations, and a 'burn-in' period of 25,000 iterations for each stem. Prior distributions assumed equal uptake from each potential source. To test the sensitivity of mixing model outputs to prior distribution selection, we repeated the mixing model analysis using a weighted prior distribution describing 70 % uptake from precipitation weighted by month according to monthly cumulative precipitation, and 10 % uptake from each potential source of groundwater, irrigation, and wastewater (SI Table 1). We assumed no isotopic fractionation during water uptake (Dawson and Ehleringer, 1992). All statistical analysis was conducted using R version 4.1 (R Core Team, 2021).

Recent studies have demonstrated a potential methodological bias in δ^2H estimation from the extraction of stem water via cryogenic vacuum distillation (Chen et al., 2020; Allen and Kirchner, 2022). As a robustness check for our mixing model outputs, we conducted an additional analysis by applying a deuterium correction to the stem δ^2H values. A range of values describing the potential offset have been reported across species, however, due to insufficient data on biases associated with *Acer platanoides*, we applied a correction of +8.1 ‰ to the stem δ^2H values as in Marx et al. (2022), representing the mean value reported in Chen et al. (2020) as a reasonable approximation of a potential offset (SI Table 1). Allen and Kirchner (2022) identify a deuterium correction of +6.1 ± 3.4 ‰ as a reasonable indication of potential bias, supporting our applied correction of +8.1 ‰.

3. Results

3.1. Weather trends and characterization of local meteoric water line

The year 2021 was a much wetter than average year in Boston. Annual precipitation was 1408 mm, 27.1 % above the 30-year average, with JJA precipitation being 621 mm, 135 % higher than average. During the sampling period from June 1 to September 14, 724 mm of rain fell, with July representing the wettest month of the sampling period and year, accounting for 315 mm of rain (Fig. 2). On July 9, tropical storm Elsa passed over Boston and produced approximately 70 mm of rain at the weather station during the July 9, 2021 sampling event. There were no significant trends over time in the daily average temperature ($p > 0.05$) or daily average relative humidity ($p > 0.05$) during the sampling period, with a mean daily temperature of 22.6 °C ($\sigma = 3.4$ °C) and mean daily relative humidity of 74.4 % ($\sigma = 11.8$ %).

The equation for best fit LMWL estimated from precipitation measurements collected between May and October 2021 was $\delta^2H = 8.7 * \delta^{18}O + 8.5$ (Fig. 3). While the LMWL slope is slightly greater than that of the global meteoric water line (GMWL; 8) and the LMWL intercept is less than that of the GMWL (10), the LMWL slope and intercept are consistent with other LMWLs estimated in continental climates at a similar latitude (Putman et al., 2019). Clear seasonal trends of isotopic enrichment of precipitation during summer months (Barbeta et al., 2018) were not observed during the sampling period, potentially due to limited sampling frequency. We observed precipitation isotopic values of a similar magnitude during May, (=−38.8 ± 0.6 ‰ for δ^2H and =−8.0 ± 0.4 ‰ for $\delta^{18}O$), June (−52.0 ± 1.0 ‰ for δ^2H and −6.7 ± 0.2 ‰ for $\delta^{18}O$) and September (−47.2 ± 4.2 ‰ for δ^2H and −5.0 ± 0.8 ‰ for $\delta^{18}O$) and relatively enriched values during August (−7.7 ± 5.8 ‰ for δ^2H and −1.9 ± 0.6 ‰ for $\delta^{18}O$; Fig. 4). Precipitation δ^2H and $\delta^{18}O$ values in July were relatively depleted (mean = −74.7 ± 2.8 ‰ for δ^2H and mean = −9.23 ± 0.2 ‰ for $\delta^{18}O$; Fig. 4), likely due to the influence of tropical storm Elsa. Tropical cyclones are known to produce extremely negative isotopic values (Lawrence and Gedzelman, 1996).

3.2. Groundwater, irrigation, and wastewater isotope ratios

Groundwater, irrigation, and wastewater isotopic values plotted along the LMWL (Fig. 3) and were isotopically distinct for each month and location used in the mixing models. Wastewater and irrigation, which both move through the city in belowground pipes and partially originate from the same source, were isotopically distinct ($p < 0.05$), with more enriched values for irrigation water (−52.8 ± 8.0 ‰ for δ^2H and −7.3 ± 0.2 ‰ for $\delta^{18}O$) compared to wastewater (−60.8 ± 6.7 ‰ for δ^2H and −8.3 ± 0.4 ‰ for $\delta^{18}O$). Wastewater and irrigation isotopic values were relatively depleted in July (SI Fig. 1), potentially due to the influence of tropical storm Elsa, but were otherwise less variable than groundwater and precipitation during the sampling period (Fig. 4). Groundwater isotopic values varied across space and time and generally followed patterns in precipitation, with the most depleted values observed in July (−71.8 ± 5.7 ‰ for δ^2H and −7.8 ± 0.4 ‰ for $\delta^{18}O$) and most enriched values in August (−51.7 ± 5.5 ‰ for δ^2H and −7.0 ± 0.4 ‰ for $\delta^{18}O$; Fig. 4).

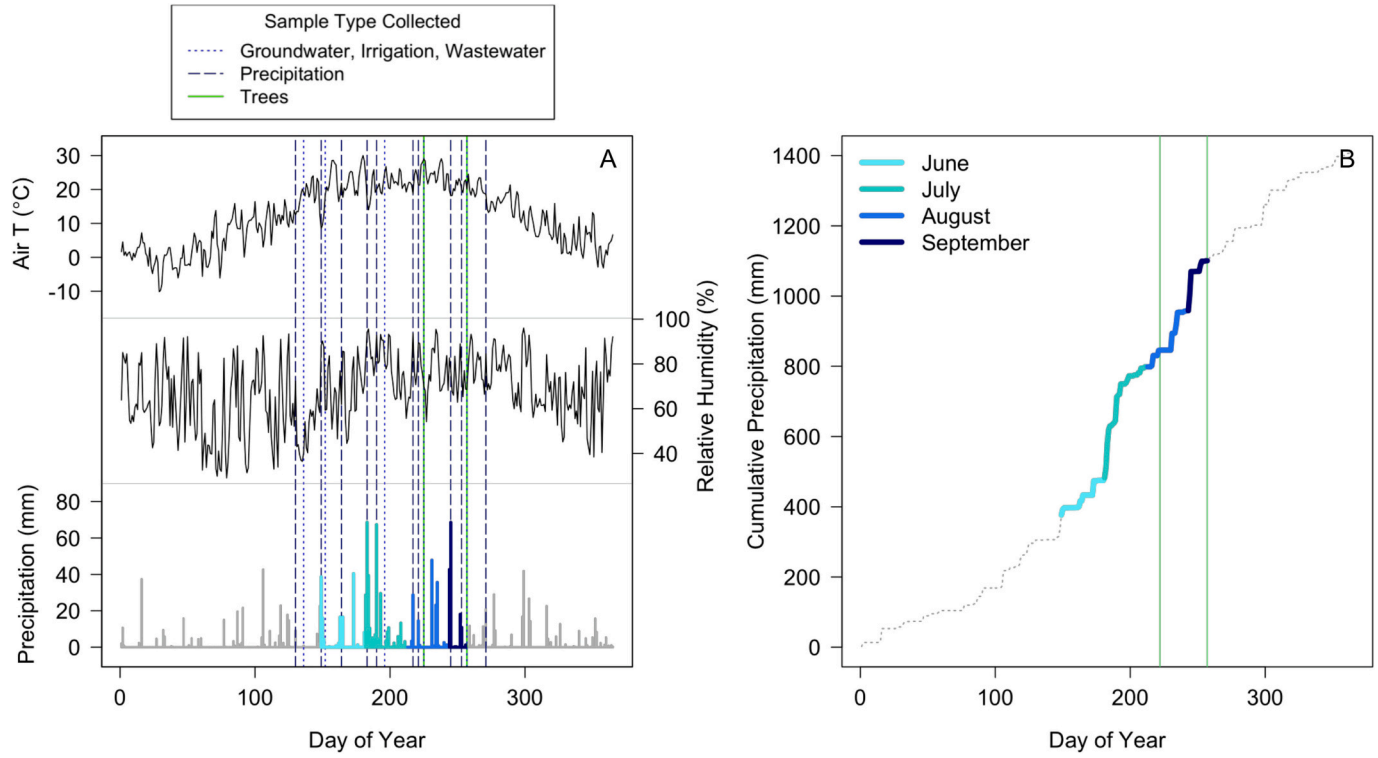

Fig. 2. (A) Daily mean air temperature (°C), daily mean relative humidity (%), and daily total precipitation (mm) for each day of 2021 measured at the weather station. Vertical lines represent water and tree sampling events. Daily total precipitation is color coded by month (legend in panel B) for the days included in the mixing model analysis. (B) Cumulative precipitation during 2021 where the time period included in the mixing model analysis is color coded by month and green vertical lines represent the days of tree stem sampling.

3.3. Stem water isotope ratios

Stem water isotopic values consistently plotted below the LMWL, indicating tree water uptake of evaporated soil water. Aggregate two-dimensional isotope values were significantly different across sampling events ($p < 0.05$; 2-Dimensional Kolmogorov-Smirnov test). Mean δ^2H values across all trees were -42.5 ± 6.3 ‰ in August and -39.8 ‰ $\pm$ 6.0 ‰ in September (Fig. 3). Mean $\delta^{18}O$ values across all trees were 4.3 ± 2.2 ‰ in August and 3.8 ± 1.7 ‰ in September (Fig. 3). After applying the evaporation line correction, the stem water isotope values were not significantly different across sampling events ($p > 0.05$). Mean evaporation line corrected δ^2H values across all trees were -70.2 ± 6.2 ‰ in August and -69.9 ‰ $\pm$ 5.5 ‰ in September (Fig. 3 inset). Mean $\delta^{18}O$ values across all trees were -8.2 ± 1.0 ‰ in August and $-8.1 \pm$ 0.9 ‰ in September (Fig. 3 inset). Aggregate isotope LC_{xs} values were not significantly different across sampling events ($p > 0.05$), indicating uptake of water exposed to a similar amount of evaporation for both sampling events. The mean LC_{xs} of water extracted from trees sampled in August was -88.2 ($\sigma = 39.5$) and -81.7 ($\sigma = 29.5$) in September.

3.4. Water source partitioning

Gelman-Rubin convergence diagnostics (Gelman and Rubin, 1992) confirmed MCMC model convergence for all Bayesian multisource mixing models used to estimate water source partitioning for each stem sample and sampling date. Example model inputs, including the reconstructed distribution of the source mixture inferred from evaporation lines, and model outputs for a tree sample collected from plot WB in August are provided in Fig. 5.

For the water extracted from tree stems collected in August 2021, precipitation was estimated to be the primary source of the water mixture, accounting for 72.6 ± 4.6 % of root water uptake (Fig. 6). The model estimated 8.6 ± 1.2 %, 9.0 ± 1.8 %, and 10.1 ± 2.0 % contributions from groundwater, irrigation, and wastewater, respectively; all of which are smaller than the model prior distribution assuming 16.7 % uptake from each source. Trees sampled in August primarily utilized rainwater from July, which experienced more rainfall in one month than the 30-year average seasonal rainfall for the entire summer season (JJA), with an average contribution of 52.2 % of stem water across stems and up to 80.2 % of water extracted from tree stems. Precipitation was the primary source of all 27 trees sampled in August, with 22 trees predominantly using rainwater from July and 5 trees predominantly using rainwater from August.

For the water extracted from tree stems collected in September, precipitation was also estimated to be the primary source of the water mixture, accounting for 65.6 ± 6.2 % of root water uptake (Fig. 5). The model estimated 13.4 ± 2.8 %, 9.7 ± 1.7 %, and 11.3 ± 2.1 % contributions from groundwater, irrigation, and wastewater, respectively; all of which are smaller than the model prior distribution assuming 16.7 % uptake from each source. Again, trees primarily utilized water from the extremely rainy month of July, with an average contribution of 42.1 % of stem water across stems and up to 84.0 % of water extracted from tree stems, however, we observe evidence of a small shift towards use of recent rainfall. Precipitation was the primary source of all 31 trees sampled in September, with 23 trees predominantly using rainwater from July and 8 trees predominantly using rainwater from August.

We found similar estimates of proportional street tree uptake from precipitation when conducting the mixing model analysis with the deuterium correction and weighted prior distribution (Table SI 1). For the water extracted from tree stems collected in August 2021, we estimated mean proportional uptake from precipitation to be 67.2 ± 4.4 % when applying the deuterium correction and 79.0 ± 2.7 % when using a non-corrected weighted prior distribution (describing 70 % uptake from precipitation weighted by month according to monthly cumulative precipitation, and 10 % uptake from each potential source of groundwater, irrigation, and wastewater). For the water extracted from tree

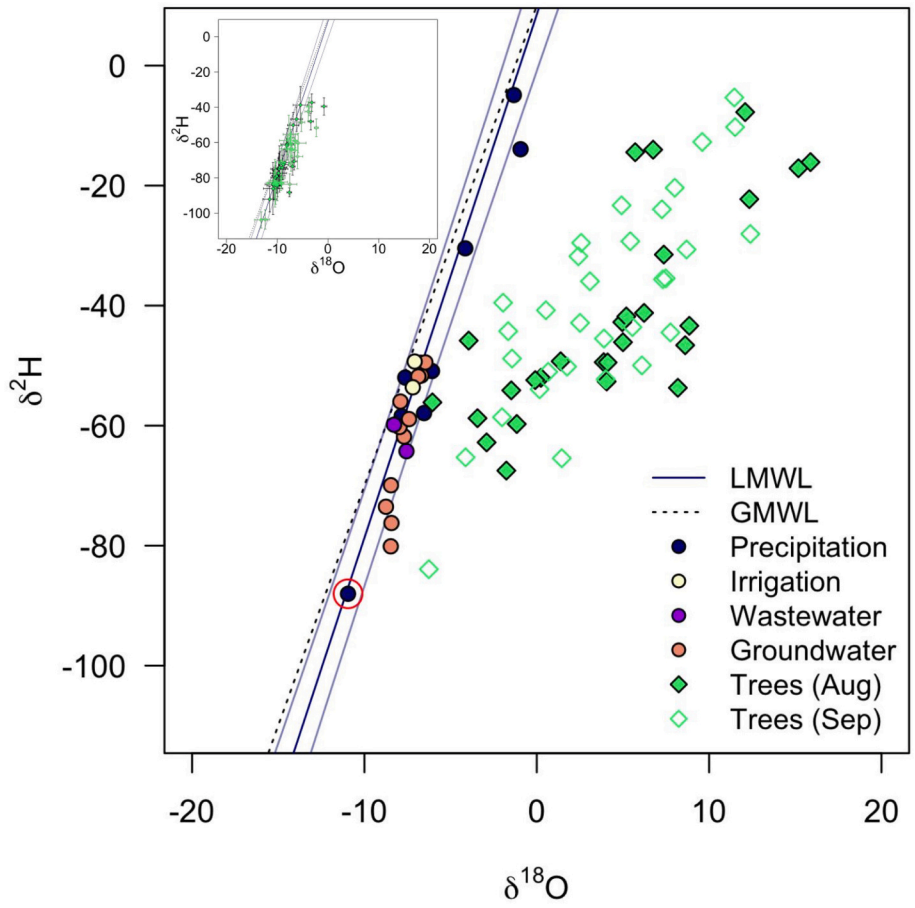

Fig. 3. Water source samples included in the mixing model analysis overlaid on the local meteoric water line (LMWL) and global meteoric water line (GMWL). Error bands on the LMWL represent a 95 % confidence interval. The precipitation sample circled in red corresponds to storm water collected during tropical storm Elsa. Green diamonds show water extracted from tree stems. Inset: Reconstructed source water mixture distributions after evaporation line correction.

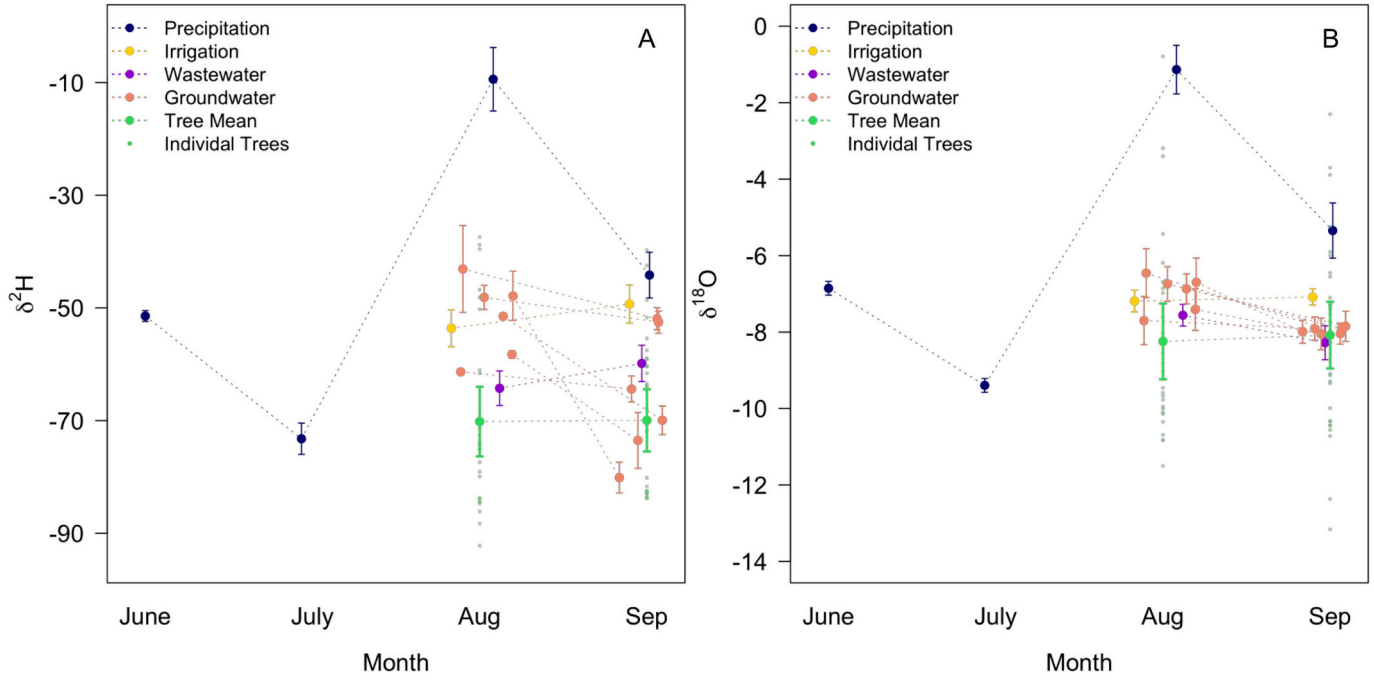

Fig. 4. Monthly (A) δ^2H and (B) $\delta^{18}O$ values (means ± 95 % CI) for each potential water source and tree stem used in the mixing model analysis, where tree stem data is presented as the reconstructed source water mixture after evaporation line correction. Points are jittered around their corresponding month of sampling on the x-axis for visual clarity.

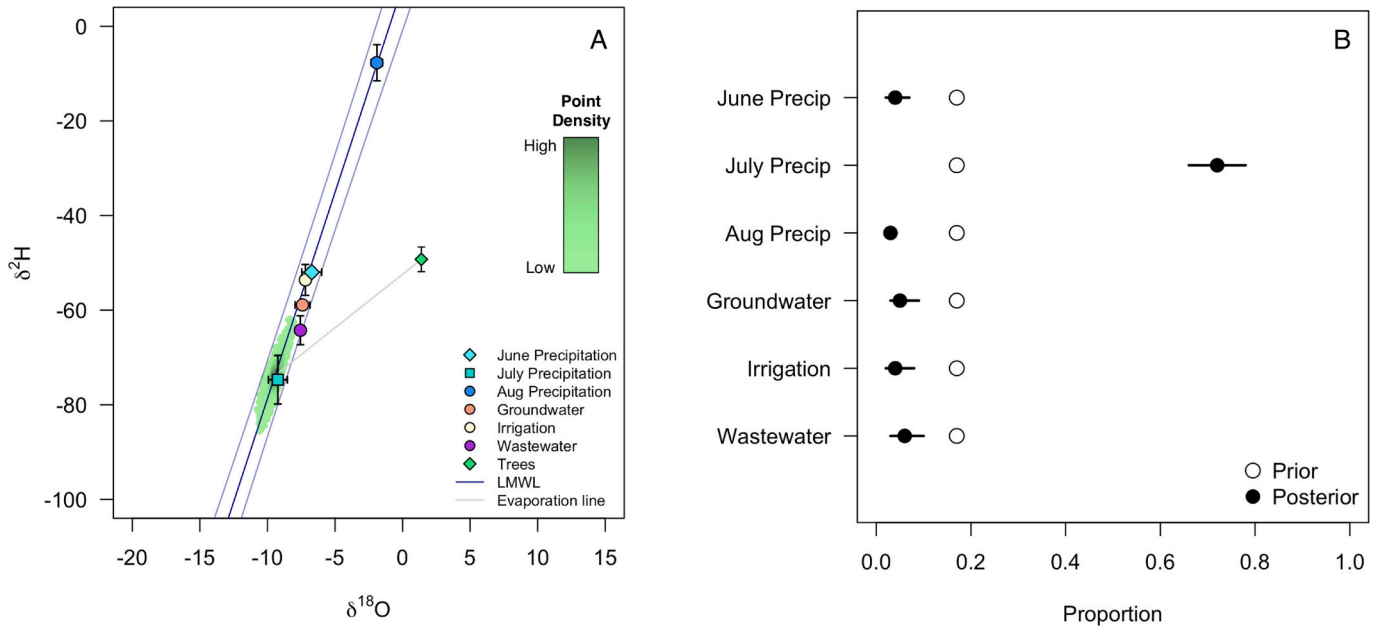

Fig. 5. (A) Example inputs into the multisource mixing model for a single tree stem sample collected in August 2021, showing how the source water mixture distribution (green point cloud) is reconstructed from an evaporation line and isotopic composition of water extracted from the tree stem (green diamond). (B) Prior estimates showing equal water uptake from each source (open circles) and model estimates of proportional water source uptake (closed circles) for the example shown in panel A, where the error bars represent the middle 50 % of estimates from 25,000 model iterations.

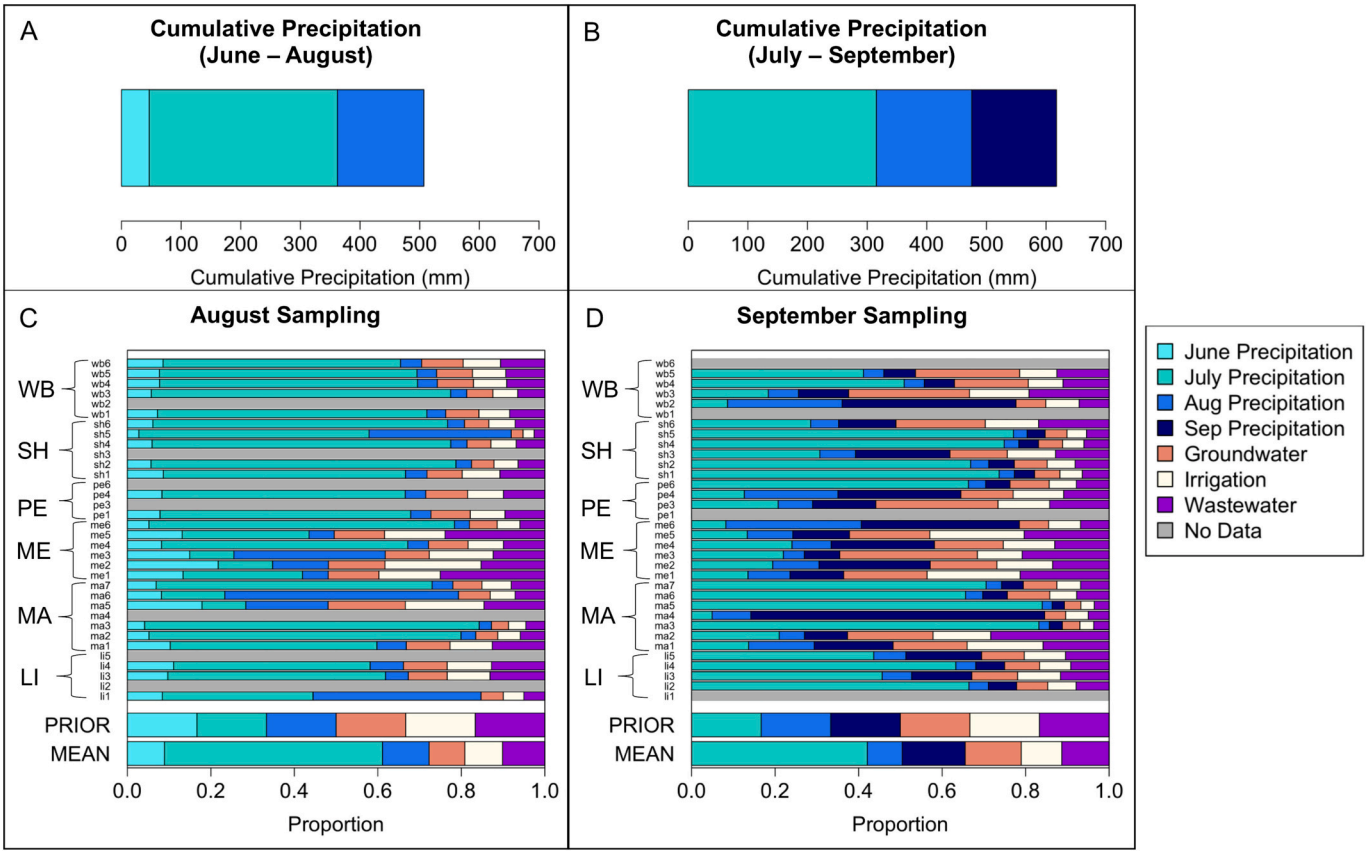

Fig. 6. (A) Cumulative precipitation (mm) for June, July, and August. (B) Cumulative precipitation (mm) for July, August, and September. (C) Mean proportional uptake from each of six potential water sources estimated from the multisource mixing model analysis for each tree sampled in August. Prior and mean posterior values are shown in the bottom two bars. (D) Mean proportional uptake from each of six potential water sources estimated from the multisource mixing model analysis for each tree sampled in September. Prior and mean posterior values are shown in the bottom two bars. Bar plots are grouped by plot, with the first two letters of the y-axis labels corresponding to the plot ID.

stems collected in September 2021, we estimated mean proportional uptake from precipitation to be 62.5 ± 4.9 % when applying the deuterium correction and 75.9 ± 4.0 % when using a non-corrected weighted prior distribution. For both August and September, the estimates derived from the mixing model with an equal uptake prior distribution and no deuterium correction fall between the estimates derived from mixing models with deuterium corrections and mixing models with weighted prior distributions. Thus, while all three mixing model variants identify precipitation as the dominant source of street tree root uptake, we report a range of values estimating the magnitude of proportional street tree water uptake attributed to precipitation.

The identification of precipitation as the dominant water source of street trees in August and September 2021 is consistent with the extremely negative LC_{xs} values observed across trees, indicating uptake of evaporated soil water. We found no relationship between tree size or growth rate (DBH and annual DBH increment, respectively) and variability in proportional uptake across sources ($p > 0.05$). We found a significant relationship between LC_{xs} and proportion of water uptake from the most recent sampled precipitation event prior to stem sampling, providing evidence that shallower rooted trees may utilize shallow soil water from recent rain events more than older, deeper soil water from previous storms. LC_{xs} may be a suitable proxy for understanding the depth at which plant roots uptake water where lower LC_{xs} values indicate more evaporation of source water and are typically found at shallower depths (Sprenger et al., 2017). The mean LC_{xs} of stem samples collected in August was −82.0 (σ = 37.9) for trees that predominantly utilized older July rainfall and −103.5 (σ = 31.5) for trees that predominantly utilized recent August rainfall. The mean LC_{xs} of stem samples collected in September was −79.7 (σ = 27.9) for trees that predominantly utilized July rainfall and −105.8 (σ = 23.1) for trees that predominantly utilized recent September rainfall.

We observed consistent proportional uptake across all six plots (Fig. 7), with precipitation being the primary water source for all street trees we examined. Differences in average tree size and localized impervious surface area did not significantly relate to variation in the proportion of precipitation taken up by trees across field plots ($p > 0.05$).

3.5. Proximity of trees to sewer lines and groundwater

The mean tree distance to the nearest sewer line ranged from 0.4 m (plot ID = ME) to 36.6 m (plot ID = MA; SI Table 2) across plots, with a median distance of 5.4 m across all sampled trees. Mean proportional wastewater uptake during the sampling period was significantly higher ($p < 0.05$) for the field plot with the shortest mean tree distance to sewer lines (plot ID = ME, μ = 15.7 %, σ = 6.5 %). The other five plots did not significantly differ in their proportional wastewater uptake ($p > 0.05$). The mean groundwater depth during the sampling period ranged from 1.0 m (plot ID = SH) to 3.7 m (plot ID = ME; SI Table 2), with a median depth of 3.5 m across all plots. Mean proportional groundwater uptake did not differ significantly across plots ($p > 0.05$).

3.6. Evapotranspiration modeling

Annual ET during 2021 in the model domains corresponding to the six field plots ranged from 256 mm yr^{-1} to 575 mm yr^{-1} with an average value of 397 mm yr^{-1} (σ = 133 mm yr^{-1}) across all plots. Mean annual ET rates in the model domains were approximately 66.1 % to 77.8 % of the 30-year Massachusetts statewide annual ET rates (510–600 mm yr^{-1}; Sanford and Selnick, 2013). Canopy cover within the model domains ranged from 19.2 % to 32.0 % with an average value of 24.7 % (σ = 5.1 %) across all plots (Fig. 8; University of Vermont Spatial Analysis Laboratory, 2020) which is less than half of the Massachusetts statewide canopy cover (57.7 %; United States Department of Agriculture Forest Service, 2019).

The fraction of precipitation lost to ET in the model domains ranged from 13.7 % to 35.3 % during August and September with an average value of 22.0 % (σ = 9.0 %) and was significantly correlated with the canopy cover within each model domain ($R^2 = 0.91$; $p = 0.003$; Fig. 8). We estimate an increase in precipitation lost to ET as 2 % for each unit increase in the percent canopy cover during August and September (Fig. 8), with a similar, significant positive relationship ($R^2 = 0.89$; $p = 0.005$) observed for the entire year (slope = 0.01, intercept = −0.16; SI Fig. 2). The mean annual proportion of precipitation lost to ET in the model domains was approximately 44.8 % to 55.0 % of the 30-year average proportion of precipitation lost to ET across the state of Massachusetts (49 %, Sanford and Selnick, 2013).

4. Discussion

In this study, we found that in the mesic City of Boston, street trees confined to tree pits predominantly use water from precipitation, rather than irrigation, groundwater, and wastewater, during a significantly wetter than average growing season. Our findings build upon those of previous studies quantifying urban tree water sourcing in semiarid ecosystems and water sourcing by trees planted in open green spaces by focusing on street trees in a city that regularly receives abundant precipitation. Urban trees located in drier environments have been shown to primarily utilize water from irrigation, with small contributions from precipitation (Bijoor et al., 2012; Gómez-Navarro et al., 2019). Urban

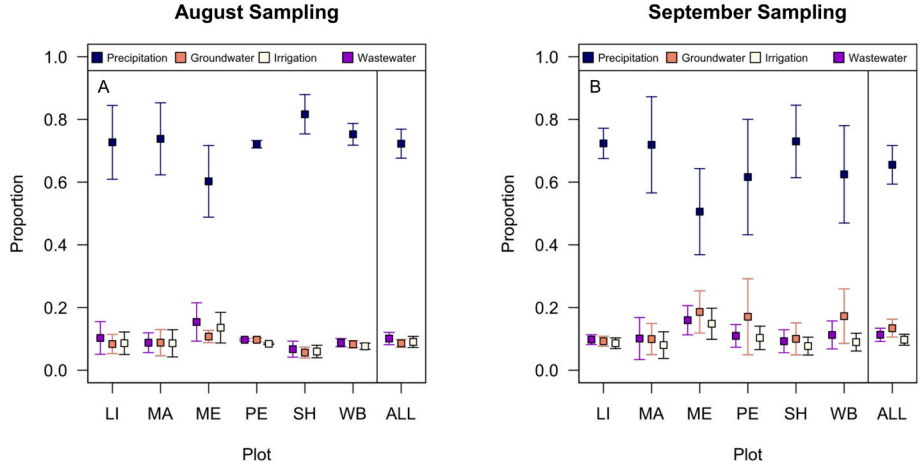

Fig. 7. (A) Mean proportional tree water uptake among trees sampled in August across plots. (B) Mean proportional tree water uptake among trees sampled in September across plots. Error bars in both panels represent 95 % confidence intervals. 'ALL' designates the mean of all trees sampled in the respective month.

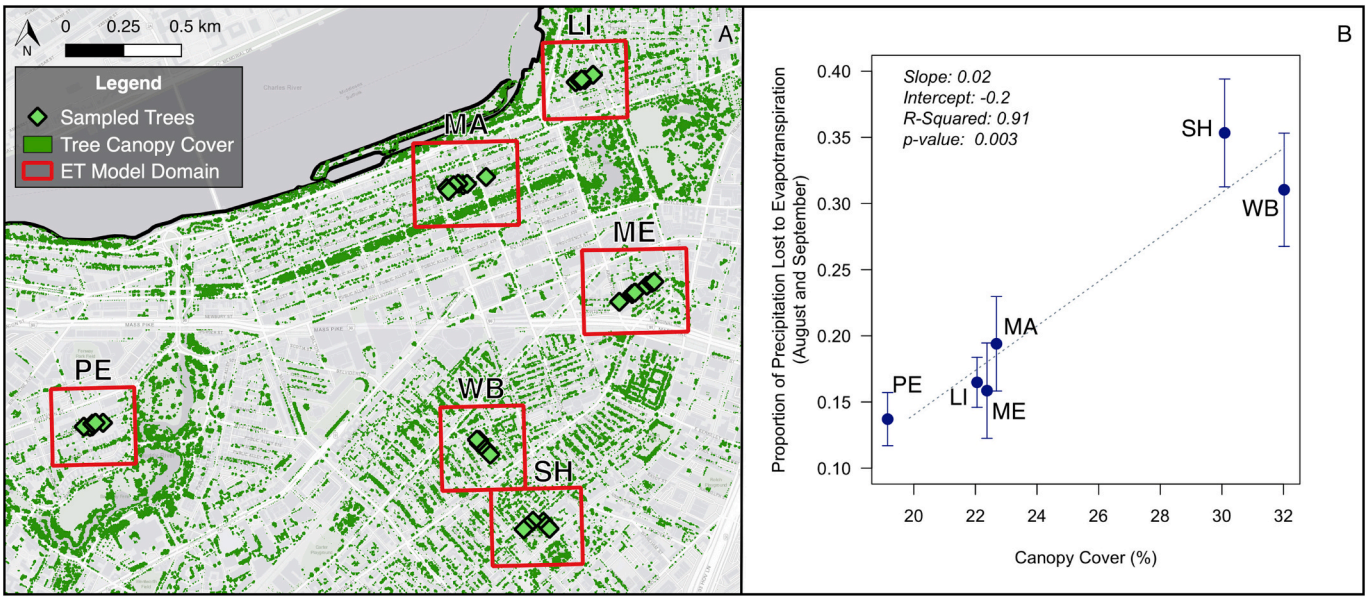

Fig. 8. (A) Spatial layout of the six ET model domains overlaid on a map of Boston's tree canopy cover (University of Vermont Spatial Analysis Laboratory, 2020) and trees sampled for isotope water source analysis in 2021. (B) Plot level proportion of precipitation lost to evapotranspiration during August and September 2021 versus plot level canopy cover. Error bars represent proportions estimated using the 95 % confidence intervals on the plot-varying proportion of water uptake from precipitation.

trees located in open green spaces and botanical gardens that are not confined to tree pits and planters have been shown to primarily utilize water from groundwater and deep soil layers (Bijoor et al., 2012; Marx et al., 2022). Here we show that despite compacted and limited soil volume inside of street tree pits and high impervious surface area fractions surrounding street tree pits, trees are able to access infiltrated storm water, with important management implications for greening initiatives that aim to expand and protect tree cover in highly paved urban areas potentially threatened by drought in a changing climate. Significant, positive relationships between canopy cover and ET, combined with the identification of water from precipitation as the primary source of street tree ET, provide support for the storm water mitigation benefits of canopy expansion initiatives.

4.1. Street trees and precipitation

All potential tree water sources identified and sampled in this study plotted along the LMWL, however, water extracted from tree stem samples plotted below the LMWL indicating tree uptake of source water mixtures that experienced evaporative fractionation. Source water evaporation prior to tree uptake is captured by extremely negative LC_{xs} values, which suggest root uptake from upper soil layers and support the mixing model outputs characterizing soil water originating from precipitation as the dominant tree water source. While we did not sample soil water from tree pits due to logistical infeasibility, the tree stem water isotope values reported in this study are consistent with the evaporatively enriched urban soil isotope values reported in Bijoor et al. (2012), which also fall well below the LMWL along a soil evaporation line. Stem water isotope values would be expected to plot closer to the LMWL if tree roots were tapping into belowground pipes or groundwater for their primary water needs. While we find limited evidence of supplemental water utilization from wastewater in trees with a close proximity to sewer lines, we find soil water primarily composed of evaporatively enriched precipitation water to be the primary water source for street trees. The Bayesian mixing model outputs suggest that storm water is adequately being captured, retained within tree pits, and made available to tree roots, even in tree pits characterized by 100% impervious surface area within a 10-meter radius (Table 1). Note that urban impervious surfaces regularly include brick pavers with spacing and cracks in the pavement that provide avenues for infiltration beyond stemflow and direct runoff into tree pits. Furthermore, our ET analysis supports the storm water mitigation benefits of tree planting initiatives as we observe a significant positive relationship between canopy cover and the proportion of precipitation lost to ET, pointing to increased citywide canopy cover as a potential way to reduce alternative avenues of precipitation loss such as runoff.

Over 50 % of land area in Boston is covered by buildings, roads, or other paved surfaces (Smith et al., 2023), expediting surface runoff to storm drains and water bodies, while reducing the amount of water made available to vegetation. Our results demonstrate that trees and tree pits can capture and direct some fraction of precipitation into soil reservoirs accessible by tree roots. Branches and leaves composing street tree crowns likely intercepted rainwater as it fell and directed the water towards the bole which accommodated stemflow down to the base of the tree, where storm water was able to enter the soil via infiltration. Studies quantifying storm water interception by deciduous broadleaf street trees report interception rates of 14–25 % of rainfall on the tree canopy (Xiao et al., 2000; Xiao and McPherson, 2011). Urban deciduous broadleaf stemflow rates of up to 22.8 % of rainfall on the tree canopy have been observed (Carlyle-Moses and Schooling, 2015), highlighting a key pathway for capturing rainwater for subsequent root uptake. Open grown trees, such as those sampled in this study, tend to have larger crown volumes due to a lack of competition for sunlight (Smith, 1996) and therefore can intercept more rainwater on a per tree basis than trees in rural woodland settings (Asadian and Weiler, 2009).

In addition to intercepting storm water in the tree canopy and directing captured water to the tree base via stemflow, tree roots are able to increase the infiltration and percolation capacity of soils through their rooting structure and transpiration, potentially contributing to the high precipitation utilization observed in this study. Urban soils are generally more compacted than rural soils in order to provide enough stability to support structures, roads, and pavement, leading to reduced infiltration rates (Gregory et al., 2006) from the compaction of macropores that could otherwise store and conduct water (Scheyer and Hipple, 2005). Tree roots within urban soils generate channels that promote infiltration of storm water. Bartens et al. (2008) found compacted soils with tree roots increased infiltration rates by 63 % relative to control soils exposed to compaction without tree roots. Armson et al. (2013)

found street trees to be effective in reducing surface runoff as trees and their associated tree pits surrounded by asphalt reduced runoff by as much as 62 % relative to 100 % asphalt surfaces, which the authors attributed to increased infiltration of soils within the tree pits. Through transpiration, tree roots increase soil pore space by removing water from soil pores, thus allowing space for subsequent storm water to infiltrate soil and fill vacated pores (Kuehler et al., 2017). Furthermore, anthropogenic manipulation of tree pits can encourage storm water runoff infiltration into urban soils. For example, the City of Boston's Complete Streets Guidelines (2013) for street tree pits advise installers to "pitch the sidewalk toward the tree pit to use storm water for irrigation," representing another potential mechanism for the availability of precipitation for street trees within tree pits.

Altogether, our data provide evidence for the storm water mitigation function of street trees as they utilize water from precipitation and their canopy cover is associated with increases in the proportion of precipitation lost to ET. However, our observations are limited to an exceptionally rainy growing season, posing questions for street tree water use under drier conditions.

4.2. Considerations regarding anomalous rainfall

The annual cumulative rainfall in Boston during 2021 was in the 86th percentile for the city dating back to 1936 (National Center for Environmental Information, 2023b), indicating that our study was conducted during a much wetter than average summer and year. While we did not measure soil moisture in this study, the high frequency of rainfall combined with several large rain events likely resulted in relatively high soil moisture levels, increased soil water potential (Bréda et al., 1995), and likely resulted in an energetically inexpensive pathway for shallow street tree roots to take up infiltrated rainwater throughout the growing season. Between the sample period of June 1–September 14, precipitation was recorded on 50 out of 106 days, including 14 consecutive days between June 30 and July 13. The longest period without rainfall lasted for only eight days between August 11 and August 18. In our analysis, we used monthly isotopic means and standard deviations from two precipitation samples per month to capture variability in soil water inputs originating from precipitation. Additionally, we consider precipitation from multiple months as potential tree water sources to consider root uptake of soil water mixtures that may be composed of both recent and previous rain events. Schütt et al. (2022) found the most important predictor of soil water potential within street tree pits of Hamburg, Germany was the 10-day rainfall sum, where rewetting events during an extraordinarily wet year resulted in soil water availability above a critical threshold defining the point at which stomatal closure from water stress would occur. In contrast, during dry years, soil water availability fell below the critical threshold for several months. Thus, it is possible that tree water source utilization might differ from the observations in this study during dry periods.

Water availability and drought can impose a strong control on rooting profiles and depth of root water uptake, and therefore may influence the sources from which street trees acquire water under dry growing conditions. In the semiarid climate of New Mexico, United States, *Pinus edulis* shifted from shallow water sources replenished by rainfall towards deeper sources in response to a drier than average summer (Grossiord et al., 2017). In the Mediterranean climate of Fontaine de Vaucluse, France, *Abies alba*, *Fagus sylvatica*, and *Quercus ilex* all utilized deep water sources more intensively during drier years (Carrière et al., 2020). In the mesic climate of New Hampshire, United States, *Acer rubrum* shifted from utilization of shallow soil water sources (0–10 cm) early in the growing season to deeper soil water sources (90–100 cm) late in the growing season corresponding to shifts in soil water availability over the growing season (Harrison et al., 2020). While our results point to uptake of shallow soil water replenished by regular rainfall, it remains unclear which deeper water sources may be available for street trees under conditions that preclude shallow soil water uptake. We note that estimated groundwater utilization increased from 8.6 ± 1.2 % to 13.4 ± 2.8 % between August and September, potentially relating to reductions in precipitation rates during August and September relative to the exceptionally rainy month of July.

4.3. Management implications

Our findings that street trees in a mesic city take up most of their water from precipitation and that canopy cover correlates strongly with ET highlight important considerations for cities managing their green infrastructure in a changing climate. The increased ET associated with increases in canopy cover demonstrates the value of management strategies that incorporate tree planting to expand canopy cover. Increases in transpiration result in a higher provision of cooling benefits through latent heat flux and a greater loss of precipitation to ET when the source water for transpiration is primarily from precipitation, given that urban trees have sufficient water resources to support their water demand. The use of green infrastructure to mitigate stormwater often focuses on larger scale solutions such as bioretention areas, permeable pavements, and green roofs. The results described here support street tree canopy expansion as an additional solution towards stormwater mitigation, with numerous co-benefits for urban communities.

In mesic cities that currently rely on precipitation to meet the water demand of their street tree population, our results show that in wet years trees are likely to meet their needs for water without irrigation. The City of Boston currently provides irrigation for newly planted street trees (of approximately 5 cm DBH) every two weeks during the growing season for two years (City of Boston, 2022b). After two years, the trees are no longer provided with regular irrigation by the City, potentially contributing to the observed street tree mortality rate in Boston of 3.1 % yr^{-1} (Smith et al., 2019).

Mean annual temperature and precipitation in the northeastern United States are projected to increase through the end of the twenty-first century (Picard et al., 2023). Despite projected increases in total annual precipitation trends, warmer temperatures may shorten the timeframe of drought-induced tree mortality such that under warmer conditions, droughts of shorter duration may be sufficient to cause widespread die-off (Adams et al., 2009), exacerbating the impact of dry years on tree health in a warmer climate. Although the trees sampled in this study experienced the highest amount of growing season (April – October) precipitation dating back to 1936 (1056.1 mm, Fig. 9), growing season rainfall during the following year (2022) was in the 5th percentile of historical growing season precipitation rates at 379.5 mm (Fig. 9), which is lower than the mean annual evaporative demand estimated in this study (397.3 mm yr^{-1}). Therefore, during dry years, the proportion of precipitation lost to ET may reflect typical trends observed in arid and semiarid ecosystems, where ET consumes nearly all precipitation. Future research in regions like the northeastern United States investigating street tree water sources during years where evaporative demand exceeds precipitation will help to elucidate whether irrigation of mature trees or other water retention strategies may be required to sustain street tree health.

Alternative management strategies to promote water access by tree roots include mulching and additional herbaceous plant cover. Compared to bare soil, soil moisture levels in upper soil layers are observed to be higher after mulch application (Wang et al., 2021) or concurrent planting of herbaceous plants (Rafi and Kazemi, 2021). Moreover, passive irrigation of street trees through harvesting and redirecting of storm water towards tree pits can accelerate tree growth and facilitate runoff reduction benefits of urban greenspace (Thom et al., 2022). Altogether, we provide evidence to suggest that while street tree water availability in arid and semiarid cities is known to require supplementation via anthropogenic irrigation, mesic cities that currently rely on adequate annual precipitation for irrigation should consider alternative water management strategies in order to support sustained benefits from street trees during prolonged dry periods.

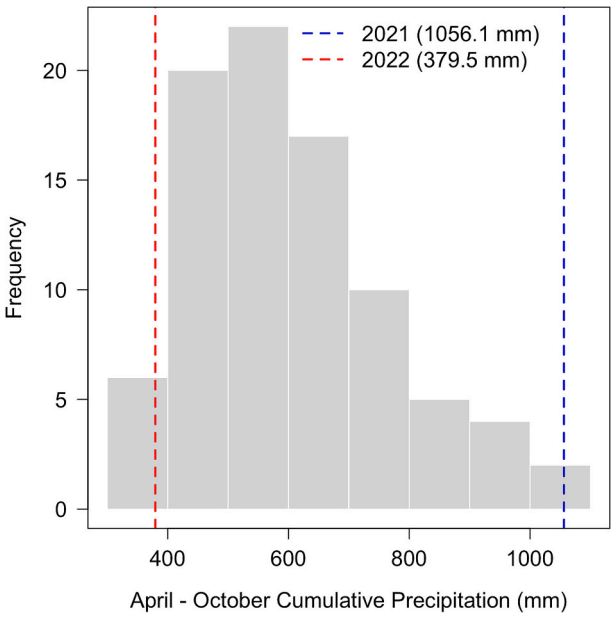

Fig. 9. Histogram of historical growing season (April – October) precipitation in Boston between 1936 and 2022. The blue line shows the value for the extremely wet year of 2021 and the red line shows the values for the relatively dry year of 2022.

4.4. Potential limitations of water source partitioning

The street tree water sources investigated here have plausible pathways for tree root access and uptake, however, without knowledge of the vertical and horizontal rooting structure of sampled trees, we cannot verify the extent to which each source was available for each individual tree. Street trees that utilized water from sources not considered here represent an unaccounted-for source of uncertainty in the analysis. We justify the inclusion of these potential urban water sources in the analysis as *Acer platanoides* has a shallow, invasive rooting system that is known to expand beyond the confines of tree pits (Gilman and Watson, 2014). Despite the shallow rooting of *Acer platanoides*, the anthropogenic barriers around street trees may force roots to grow at greater depths (Mullaney et al., 2015) with other *Acer* spp. rooting depths observed to be >2 m in natural ecosystems (Haag et al., 1989).

The potential for water uptake from wastewater sources was assessed by estimating the horizontal distance from street tree boles to the nearest sewer line, however, the individual sewer line depth is unknown, precluding our ability to confirm root access. Sewer mains in Boston are located a minimum of 2.3 m below the ground surface with connections to buildings located at the bottom of building foundations (approximately equal to the Boston City Base Datum of 1.72 m below the surface) through downward sloping pipes to the sewer main (Boston Water and Sewer Commission, 2016). Wastewater is assumed to be a potential water source as root intrusion in sewer systems is a well-documented phenomenon. Rolf and Stål (1994) found up to 14 root intrusions per km in sewer lines of Malmo, Sweden and Cameron et al. (2017) found up to 80 % of sewer blockages across Sydney, Australia attributable to tree root intrusion. Future research may incorporate additional methods, such as the use of CCTV data, to validate the occurrence of sewer line root infiltration by sampled trees.

Groundwater sources represent the deepest potential water source, with a mean depth of 3.1 m across plots, and may not be accessible to shallow rooted trees sampled in this study. This could lead to potential overestimation of street tree groundwater utilization. Urban trees have been demonstrated to utilize groundwater sources (Bijoor et al., 2012; Marx et al., 2022), although the potential for utilization from street trees remains unclear.

None of the trees included in this analysis are irrigated by the City of Boston. During sampling, evidence of potential pathways for irrigation application via sprinklers and hoses were observed in adjacent residential yards.

Altogether, the water sources included in this analysis are potentially accessible by street trees. The prior assumption that all sources are available for each tree does limit the interpretation of the water source partitioning analysis by potentially estimating source water contributions from sources that were absent in the water mixture taken up by street trees. Furthermore, our analysis is dependent on water source sampling methods that are representative of all potential water sources. We quantified monthly variability in the isotopic composition of precipitation by using monthly means and standard deviations of two rain events per month as source inputs in the Bayesian mixing model analysis but did not collect samples from all rain events during the study period. Rain events contributing to soil water isotopic composition that were not sampled, or water sources accessible by tree roots other than precipitation, irrigation, groundwater, and wastewater, represent an unaccounted-for source of uncertainty in the analysis. Additionally, the short time series of tree stem water extractions limits our ability to estimate variability in water source utilization over time, particularly during prolonged dry periods.

The Bayesian modeling approach utilized in this study has been demonstrated to accurately identify primary sources within a mixture, with the constraint that estimated proportional uptake from non-primary sources cannot be zero (Litmanen et al., 2020; Guerrero and Rogers, 2020). Therefore, low proportional source attribution may also indicate the absence of a source within the water mixture. We report a range of proportional uptake from precipitation (62.5–79.0 %) by repeating the analysis for a range of prior distributions. The residual estimates of irrigation, wastewater, and groundwater contributions may indicate the absence of one or more sources in the water mixture, limiting interpretation of the magnitude of non-primary water source utilization.

5. Conclusions

Our results show that in contrast to the findings of previous work in arid and semiarid, irrigated urban ecosystems, street trees in a mesic city that does not provide regular irrigation predominantly utilized water from precipitation during a wet year. The observed utilization of precipitation from street trees in tree pits supports the tree planting benefits of runoff reduction via soil infiltration and a higher fraction of precipitation lost to the atmosphere via ET with increasing canopy cover, however, the dependency of street trees on precipitation may reduce their drought resilience. This study highlights a need for future research on street tree water source partitioning in mesic cities during dry conditions as cities work to efficiently manage their water resources, while simultaneously maximizing the benefits of the urban forest in a changing climate.

CRediT authorship contribution statement

Ian A Smith: Conceptualization; Data curation; Formal analysis; Funding acquisition; Investigation; Methodology; Visualization; Roles/Writing – original draft; Writing – review & editing

Pamela H. Templer: Conceptualization; Funding acquisition; Investigation; Methodology; Project administration; Supervision; Visualization; Roles/Writing – original draft; Writing – review & editing

Lucy R. Hutyra: Conceptualization; Funding acquisition; Investigation; Methodology; Project administration; Supervision; Visualization; Roles/Writing – original draft; Writing – review & editing

Declaration of competing interest

The authors declare that they have no known competing financial

interests or personal relationships that could have appeared to influence the work reported in this paper.

Data availability

The data for this study can be found at: "Water sources for street trees in mesic urban environments", https://doi.org/10.7910/DVN/Z3GLO1, Harvard Dataverse.

Acknowledgements

Financial support for this research was provided by an Early-Stage Urban Research Award from the Boston University Initiative on Cities, a National Science Foundation (NSF) Graduate Research Fellowship to Smith (DGE-1840990), an NSF Research Traineeship (NRT) grant to Boston University (DGE-1735087), and NSF grant ICER-1854706. We thank Robert Michener and the Boston University Stable Isotope Laboratory for isotope sample processing, Hristiana Stoynova and Joy Winbourne for assistance with field data collection, Jamie Harrison for guidance in coding and statistical methodology, and the Boston Groundwater Trust for providing access to groundwater observation wells.

Appendix A. Supplementary data

Supplementary data to this article can be found online at https://doi.org/10.1016/j.scitotenv.2023.168411.

References

Adams, H.D., Guardiola-Claramonte, M., Barron-Gafford, G.A., Villegas, J.C., Breshears, D.D., Zou, C.B., Troch, P.A., Huxman, T.E., 2009. Temperature sensitivity of drought-induced tree mortality portends increased regional die-off under global-change-type drought. Proc. Natl. Acad. Sci. 106 (17), 7063–7066. https://doi.org/10.1073/pnas.0901438106.

Allen, S.T., Kirchner, J.W., 2022. Potential effects of cryogenic extraction biases on plant water source partitioning inferred from xylem-water isotope ratios. Hydrol. Process. 36 (2) https://doi.org/10.1002/hyp.14483.

Allison, G.B., Barnes, C.J., Hughes, M.W., 1983. The distribution of deuterium and 18O in dry soils 2. Experimental. J. Hydrol. 64 (1), 377–397. https://doi.org/10.1016/0022-1694(83)90078-1.

Amin, A., Zuecco, G., Marchina, C., Engel, M., Penna, D., McDonnell, J.J., Borga, M., 2021. No evidence of isotopic fractionation in olive trees (Olea europaea): a stable isotope tracing experiment. Hydrol. Sci. J. 66 (16), 2415–2430. https://doi.org/10.1080/02626667.2021.1987440.

Armson, D., Stringer, P., Ennos, A.R., 2013. The effect of street trees and amenity grass on urban surface water runoff in Manchester, UK. Urban Forest. Urban Green. 12 (3), 282–286. https://doi.org/10.1016/j.ufug.2013.04.001.

Asadian, Y., Weiler, M., 2009. A new approach in measuring rainfall interception by urban trees in coastal British Columbia. Water Quality Res. J. 44 (1), 16–25. https://doi.org/10.2166/wqrj.2009.003.

Balugani, E., Lubczynski, M.W., Reyes-Acosta, L., van der Tol, C., Francés, A.P., Metselaar, K., 2017. Groundwater and unsaturated zone evaporation and transpiration in a semi-arid open woodland. J. Hydrol. 547, 54–66. https://doi.org/10.1016/j.jhydrol.2017.01.042.

Barbeta, A., Ogée, J., Peñuelas, J., 2018. Stable-isotope techniques to investigate sources of plant water. In: Sánchez-Moreiras, A.M., Reigosa, M.J. (Eds.), Advances in Plant Ecophysiology Techniques. Springer International Publishing, pp. 439–456. https://doi.org/10.1007/978-3-319-93233-0_26.

Bartens, J., Day, S.D., Harris, J.R., Dove, J.E., Wynn, T.M., 2008. Can urban tree roots improve infiltration through compacted subsoils for stormwater management? J. Environ. Qual. 37 (6), 2048–2057. https://doi.org/10.2134/jeq2008.0117.

Benettin, P., Volkmann, T.H.M., von Freyberg, J., Frentress, J., Penna, D., Dawson, T.E., Kirchner, J.W., 2018. Effects of climatic seasonality on the isotopic composition of evaporating soil waters. Hydrol. Earth Syst. Sci. 22 (5), 2881–2890. https://doi.org/10.5194/hess-22-2881-2018.

Bijoor, N.S., McCarthy, H.R., Zhang, D., Pataki, D.E., 2012. Water sources of urban trees in the Los Angeles metropolitan area. Urban Ecosyst. 15 (1), 195–214. https://doi.org/10.1007/s11252-011-0196-1.

Birkel, C., Helliwell, R., Thornton, B., Gibbs, S., Cooper, P., Soulsby, C., Tetzlaff, D., Spezia, L., Esquivel-Hernández, G., Sánchez-Murillo, R., Midwood, A.J., 2018. Characterization of surface water isotope spatial patterns of Scotland. J. Geochem. Explor. 194, 71–80. https://doi.org/10.1016/j.gexplo.2018.07.011.

Boston Groundwater Trust, 2021. Boston Groundwater Trust Observation Well and Building Foundation Information Center. Available from: https://experience.arcgis.com/experience/7eb90a8897db487481a7e915e68a0630.

Boston Water and Sewer Commission, 2016. Common Trench for Water and Sewer Services. https://www.bwsc.org/sites/default/files/2019-01/b-10_-_common_trench_for_water_and_sewer_services.pdf.

Bowen, G., 2022. isoWater: Discovery, Retrieval, and Analysis of Water Isotope Data (R package version 1.0.1.9000).

Bowler, D.E., Buyung-Ali, L., Knight, T.M., Pullin, A.S., 2010. Urban greening to cool towns and cities: a systematic review of the empirical evidence. Landsc. Urban Plan. 97 (3), 147–155. https://doi.org/10.1016/j.landurbplan.2010.05.006.

Bréda, N., Granier, A., Barataud, F., Moyne, C., 1995. Soil water dynamics in an oak stand. Plant and Soil 172 (1), 17–27. https://doi.org/10.1007/BF00020856.

Cameron, B., McGowan, M., Mitchell, C., Winder, J., Kerr, R., Zhang, M., 2017. Predicting sewer chokes through machine learning. Water E-J. 2 (4), 1–13. https://doi.org/10.21139/wej.2017.035.

Carlyle-Moses, D.E., Schooling, J.T., 2015. Tree traits and meteorological factors influencing the initiation and rate of stemflow from isolated deciduous trees. Hydrol. Process. 29 (18), 4083–4099. https://doi.org/10.1002/hyp.10519.

Carrière, S.D., Martin-StPaul, N.K., Cakpo, C.B., Patris, N., Gillon, M., Chalikakis, K., Doussan, C., Olioso, A., Babic, M., Jouineau, A., Simioni, G., Davi, H., 2020. The role of deep vadose zone water in tree transpiration during drought periods in karst settings – insights from isotopic tracing and leaf water potential. Sci. Total Environ. 699, 134332 https://doi.org/10.1016/j.scitotenv.2019.134332.

Chen, Y., Helliker, B.R., Tang, X., Li, F., Zhou, Y., Song, X., 2020. Stem water cryogenic extraction biases estimation in deuterium isotope composition of plant source water. Proc. Natl. Acad. Sci. 117 (52), 33345–33350. https://doi.org/10.1073/pnas.2014422117.

City of Boston, 2013. Boston Complete Streets Design Guidelines. https://www.boston.gov/departments/transportation/boston-complete-streets.

City of Boston, 2021. Caring for Boston's Urban Forest. https://www.boston.gov/caring-bostons-urban-forest.

City of Boston, 2022a. Urban Forest Plan. https://www.boston.gov/departments/parks-and-recreation/urban-forest-plan.

City of Boston, 2022b. How to Get A Tree Planted On City Land. https://www.boston.gov/departments/parks-and-recreation/how-get-tree-planted-city-land.

Dansgaard, W., 1964. Stable isotopes in precipitation. Tellus 16 (4), 436–468. https://doi.org/10.1111/j.2153-3490.1964.tb00181.x.

Dawson, T.E., Ehleringer, J.R., 1993. Isotopic enrichment of water in the "woody" tissues of plants: implications for plant water source, water uptake, and other studies which use the stable isotopic composition of cellulose. Geochim. Cosmochim. Acta 57 (14), 3487–3492. https://doi.org/10.1016/0016-7037(93)90554-A.

Dawson, T.E., Mambelli, S., Plamboeck, A.H., Templer, P.H., Tu, K.P., 2002. Stable isotopes in plant ecology. Annu. Rev. Ecol. Syst. 33 (1), 507–559. https://doi.org/10.1146/annurev.ecolsys.33.020602.095451.

Duncan, M.J., Clarke, N.D., Birch, S.L., Tallis, J., Hankey, J., Bryant, E., Eyre, E.L.J., 2014. The effect of green exercise on blood pressure, heart rate and mood state in primary school children. Int. J. Environ. Res. Public Health 11 (4), 4. https://doi.org/10.3390/ijerph110403678.

Ehleringer, J.R., Dawson, T.E., 1992. Water uptake by plants: perspectives from stable isotope composition. Plant Cell Environ. 15 (9), 1073–1082. https://doi.org/10.1111/j.1365-3040.1992.tb01657.x.

Eisenman, T.S., Churkina, G., Jariwala, S.P., Kumar, P., Lovasi, G.S., Pataki, D.E., Weinberger, K.R., Whitlow, T.H., 2019. Urban trees, air quality, and asthma: an interdisciplinary review. Landsc. Urban Plan. 187, 47–59. https://doi.org/10.1016/j.landurbplan.2019.02.010.

Ellsworth, P.Z., Williams, D.G., 2007. Hydrogen isotope fractionation during water uptake by woody xerophytes. Plant and Soil 291 (1), 93–107. https://doi.org/10.1007/s11104-006-9177-1.

Fenger, J., 1999. Urban air quality. Atmos. Environ. 33 (29), 4877–4900. https://doi.org/10.1016/S1352-2310(99)00290-3.

Food and Agriculture Organization of the United Nations, 2018. Forests and Sustainable Cities: Inspiring Stories From Around the World. FAO, Rome, Italy.

Galea, S., Vlahov, D., 2005. URBAN HEALTH: evidence, challenges, and directions. Annu. Rev. Public Health 26 (1), 341–365. https://doi.org/10.1146/annurev.publhealth.26.021304.144708.

Gelman, A., Rubin, D.B., 1992. Inference from iterative simulation using multiple sequences. Stat. Sci. 7 (4) https://doi.org/10.1214/ss/1177011136.

Gibson, J.J., Birks, S.J., Edwards, T.W.D., 2008. Global prediction of δA and δ2H-δ18O evaporation slopes for lakes and soil water accounting for seasonality. Global Biogeochem. Cycles 22 (2). https://doi.org/10.1029/2007GB002997.

Gilman, E.F., Watson, D.G., 2014. *Acer Platanoides:* Norway Maple. University of Florida, Gainesville Florida.

Gleick, P.H., Haasz, D., Henges-Jeck, C., Srinivasan, V., Wolff, G., 2003. Waste Not, Want Not: The Potential for Urban Water Conservation in California. Pacific Institute, Oakland California.

Gómez-Navarro, C., Pataki, D.E., Bowen, G.J., Oerter, E.J., 2019. Spatiotemporal variability in water sources of urban soils and trees in the semiarid, irrigated Salt Lake Valley. Ecohydrology 12 (8), e2154. https://doi.org/10.1002/eco.2154.

Gregory, J.H., Dukes, M., Jones, P., Miller, G., 2006. Effect of urban soil compaction on infiltration rate. J. Soil Water Conserv. 61, 117–124.

Grossiord, C., Sevanto, S., Dawson, T.E., Adams, H.D., Collins, A.D., Dickman, L.T., Newman, B.D., Stockton, E.A., McDowell, N.G., 2017. Warming combined with more extreme precipitation regimes modifies the water sources used by trees. New Phytol. 213 (2), 584–596. https://doi.org/10.1111/nph.14192.

Guerrero, A.I., Rogers, T.L., 2020. Evaluating the performance of the Bayesian mixing tool mixsiar with fatty acid data for quantitative estimation of diet. Sci. Rep. 10 (1) https://doi.org/10.1038/s41598-020-77396-1.

Haag, Carl L., Johnson, James E., Erdmann, Gayne G., 1989. Rooting Depths of Red Maple (*Acer Rubrum* L.) on Various Sites in the Lake States. Research Note NC-347. U.S. Dept. of Agriculture, Forest Service, North Central Forest Experiment Station, St. Paul, MN.

Harrison, J.L., Blagden, M., Green, M.B., Salvucci, G.D., Templer, P.H., 2020. Water sources for red maple trees in a northern hardwood forest under a changing climate. Ecohydrology 13 (8). https://doi.org/10.1002/eco.2248.

Jha, A.K., Bloch, R., Lamond, J., 2012. Cities and Flooding. The World Bank. https://doi.org/10.1596/978-0-8213-8866-2.

Konijnendijk, C.C., 2010. Urban Forests and Trees: A Reference Book. Springer.

Krefis, A.C., Augustin, M., Schlünzen, K.H., Oßenbrügge, J., Augustin, J., 2018. How does the urban environment affect health and well-being? A systematic review. Urban Science 2 (1), 1. https://doi.org/10.3390/urbansci2010021.

Kuehler, E., Hathaway, J., Tirpak, A., 2017. Quantifying the benefits of urban forest systems as a component of the green infrastructure stormwater treatment network. Ecohydrology 10 (3), e1813. https://doi.org/10.1002/eco.1813.

Landwehr, J.M., Coplen, T.B., 2004. Line-conditioned Excess: A New Method for Characterizing Stable Hydrogen and Oxygen Isotope Ratios in Hydrologic Systems, pp. 98–99. http://inis.iaea.org/search/search.aspx?orig_q=RN:36008379.

Lawrence, R.J., Gedzelman, D.S., 1996. Low stable isotope ratios of tropical cyclone rains. Geophys. Res. Lett. 23 (5), 527–530. https://doi.org/10.1029/96GL00425.

Litmanen, J.J., Perälä, T.A., Taipale, S.J., 2020. Comparison of Bayesian and numerical optimization-based diet estimation on herbivorous zooplankton. Philos. Trans. R. Soc., B 375 (1804), 20190651. https://doi.org/10.1098/rstb.2019.0651.

Marx, C., Tetzlaff, D., Hinkelmann, R., Soulsby, C., 2022. Seasonal variations in soil–plant interactions in contrasting urban green spaces: insights from water stable isotopes. J. Hydrol. 612, 127998 https://doi.org/10.1016/j.jhydrol.2022.127998.

Metropolitan Area Planning Council, 2021. Regional Wastewater Management. Available from: https://datacommon.mapc.org/gallery/2021/april.

Miller, G.R., Chen, X., Rubin, Y., Ma, S., Baldocchi, D.D., 2010. Groundwater uptake by woody vegetation in a semiarid oak savanna. Water Resour. Res. 46 (10) https://doi.org/10.1029/2009WR008902.

Moser, A., Rötzer, T., Pauleit, S., Pretzsch, H., 2016. The urban environment can modify drought stress of small-leaved lime (Tilia cordata mill.) and black locust (Robinia pseudoacacia L.). Forests 7 (12), 71. https://doi.org/10.3390/f7030071.

Mullaney, J., Lucke, T., Trueman, S.J., 2015. A review of benefits and challenges in growing street trees in paved urban environments. Landsc. Urban Plan. 134, 157–166. https://doi.org/10.1016/j.landurbplan.2014.10.013.

National Centers for Environmental Information, 2023a. National Centers for Environmental Information, U.S. Climate Normals. Available from: https://www.ncei.noaa.gov/access/search/data-search/normals-annualseasonal-1991-2020.

National Centers for Environmental Information, 2023b. National Centers for Environmental Information, U.S. Climate Normals. Available from: https://www.ncei.noaa.gov/access/search/data-search/global-summary-of-the-year.

Oke, T.R., 1982. The energetic basis of the urban heat island. Q. J. Roy. Meteorol. Soc. 108 (455), 1–24. https://doi.org/10.1002/qj.49710845502.

Oke, T.R., Mills, G., Christen, A., Voogt, J.A., 2017. Urban Climates. Cambridge University Press. https://doi.org/10.1017/9781139016476.

Parnell, A., 2021. simmr: A Stable Isotope Mixing Model. R package version 0.4.5. https://CRAN.R-project.org/package=simmr.

Parnell, A.C., Phillips, D.L., Bearhop, S., Semmens, B.X., Ward, E.J., Moore, J.W., Jackson, A.L., Grey, J., Kelly, D.J., Inger, R., 2013. Bayesian stable isotope mixing models. Environmetrics 24 (6), 387–399. https://doi.org/10.1002/env.2221.

Peche, A., Graf, T., Fuchs, L., Neuweiler, I., 2017. A coupled approach for the three-dimensional simulation of pipe leakage in variably saturated soil. J. Hydrol. 555, 569–585. https://doi.org/10.1016/j.jhydrol.2017.10.050.

Phillips, D.L., Inger, R., Bearhop, S., Jackson, A.L., Moore, J.W., Parnell, A.C., Semmens, B.X., Ward, E.J., 2014. Best practices for use of stable isotope mixing models in food-web studies. Can. J. Zool. 92 (10), 823–835. https://doi.org/10.1139/cjz-2014-0127.

Picard, C.J., Winter, J.M., Cockburn, C., Hanrahan, J., Teale, N.G., Clemins, P.J., Beckage, B., 2023. Twenty-first century increases in total and extreme precipitation across the Northeastern USA. Clim. Change 176 (6). https://doi.org/10.1007/s10584-023-03545-w.

Putman, A.L., Fiorella, R.P., Bowen, G.J., Cai, Z., 2019. A global perspective on local meteoric water lines: meta-analytic insight into fundamental controls and practical constraints. Water Resour. Res. 55 (8), 6896–6910. https://doi.org/10.1029/2019WR025181.

R Core Team, 2021. R: A Language and Environment for Statistical Computing. R Foundation for Statistical Computing, Vienna, Austria. URL. https://www.R-project.org/.

Rafi, Z.N., Kazemi, F., 2021. Effects of planting combinations and mulch types on soil moisture and temperature of xeric landscapes. Urban Forest. Urban Green. 58, 126966 https://doi.org/10.1016/j.ufug.2020.126966.

Randrup, T.B., McPherson, E.G., Costello, L.R., 2001. Tree root intrusion in sewer systems: review of extent and costs. J. Infrastruct. Syst. 7 (1), 26–31. https://doi.org/10.1061/(ASCE)1076-0342(2001)7:1(26).

Rolf, K., Stål, Ö., 1994. Tree roots in sewer systems in Malmo, Sweden. Arboriculture Urban Forest. 20 (6), 329–335. https://doi.org/10.48044/jauf.1994.058.

Rothfuss, Y., Javaux, M., 2016. Isotopic approaches to quantifying root water uptake and redistribution: a reviewand comparison of methods [preprint]. In: Biogeochemistry: Stable Isotopes & Other Tracers. https://doi.org/10.5194/bg-2016-410.

Sanford, W.E., Selnick, D.L., 2013. Estimation of evapotranspiration across the conterminous United States using a regression with climate and land-cover data. JAWRA J. Am. Water Resour. Assoc. 49 (2), 217–230. https://doi.org/10.1111/jawr.12049.

Scheyer, J.M., Hipple, K.W., 2005. Urban Soil Primer. United States Department of Agriculture, Natural Resources Conservation Service. National Soil Survey Center, Lincoln, Nebraska. http://soils.usda.gov/use.

Schütt, A., Becker, J.N., Gröngröft, A., Schaaf-Titel, S., Eschenbach, A., 2022. Soil water stress at young urban street-tree sites in response to meteorology and site parameters. Urban Forest. Urban Green. 75, 127692 https://doi.org/10.1016/j.ufug.2022.127692.

Seneviratne, S.I., Nicholls, N., Easterling, D., Goodess, C.M., Kanae, S., Kossin, J., Luo, Y., Marengo, J., McInnes, K., Rahimi, M., Reichstein, M., Sorteberg, A., Vera, C., Zhang, X., 2012. Changes in climate extremes and their impacts on the natural physical environment. In: Field, C.B., Barros, V., Stocker, T.F., Qin, D., Dokken, D.J., Ebi, K.L., Mastrandrea, M.D., Mach, K.J., Plattner, G.-K., Allen, S.K., Tignor, M., Midgley, P.M. (Eds.), Managing the Risks of Extreme Events and Disasters to Advance Climate Change Adaptation. Cambridge University Press, Cambridge, UK, and New York, NY, USA, pp. 109–230. A Special Report of Working Groups I and II of the Intergovernmental Panel on Climate Change (IPCC).

Shuster, W.D., Bonta, J., Thurston, H., Warnemuende, E., Smith, D.R., 2005. Impacts of impervious surface on watershed hydrology: a review. Urban Water J. 2 (4), 263–275. https://doi.org/10.1080/15730620500386529.

Smith, D.M., 1996. The Practice of Silviculture, 9th ed. Wiley.

Smith, I.A., Dearborn, V.K., Hutyra, L.R., 2019. Live fast, die young: accelerated growth, mortality, and turnover in street trees. PloS One 14 (5), e0215846. https://doi.org/10.1371/journal.pone.0215846.

Smith, I.A., Winbourne, J.B., Tieskens, K.F., Jones, T.S., Bromley, F.L., Li, D., Hutyra, L. R., 2021. A satellite-based model for estimating latent heat flux from urban vegetation. Front. Ecol. Evol. 9 https://doi.org/10.3389/fevo.2021.695995.

Smith, I.A., Fabian, M.P., Hutyra, L.R., 2023. Urban green space and albedo impacts on surface temperature across seven United States cities. Sci. Total Environ. 857, 159663 https://doi.org/10.1016/j.scitotenv.2022.159663.

South, E.C., Hohl, B.C., Kondo, M.C., MacDonald, J.M., Branas, C.C., 2018. Effect of greening vacant land on mental health of community-dwelling adults: a cluster randomized trial. JAMA Netw. Open 1 (3), e180298. https://doi.org/10.1001/jamanetworkopen.2018.0298.

Sprenger, M., Tetzlaff, D., Soulsby, C., 2017. Soil water stable isotopes reveal evaporation dynamics at the soil–plant–atmosphere interface of the critical zone. Hydrol. Earth Syst. Sci. 21 (7), 3839–3858. https://doi.org/10.5194/hess-21-3839-2017.

Thom, J.K., Fletcher, T.D., Livesley, S.J., Grey, V., Szota, C., 2022. Supporting growth and transpiration of newly planted street trees with passive irrigation systems. Water Resour. Res. 58 (1) https://doi.org/10.1029/2020WR029526 e2020WR029526.

United Nations Department of Economic and Social Affairs Population Division, 2018. World Urbanization Prospects: The 2018 Revision. United Nations, New York, NY.

United States Department of Agriculture Forest Service, 2019. NLCD Tree Canopy Cover (CONUS). Salt Lake City, UT.

University of Vermont Spatial Analysis Laboratory, 2020. High Resolution Land Cover for City of Boston, MA (2019). University of Vermont Spatial Analysis Laboratory, Burlington, VT. https://bostonopendata-boston.opendata.arcgis.com/maps/boston::canopy-change-assessment-2019-land-cover/about.

Vargas, A.I., Schaffer, B., Yuhong, L., Sternberg, L. da S.L., 2017. Testing plant use of mobile vs immobile soil water sources using stable isotope experiments. New Phytol. 215 (2), 582–594. https://doi.org/10.1111/nph.14616.

Wang, B., Niu, J., Berndtsson, R., Zhang, L., Chen, X., Li, X., Zhu, Z., 2021. Efficient organic mulch thickness for soil and water conservation in urban areas. Sci. Rep. 11 (1), 1 https://doi.org/10.1038/s41598-021-85343-x.

Wershaw, R.L., Friedman, I., Heller, S.J., Frank, P.A., 1970. Hydrogen isotopic fractionation of water passing through trees. In: Hobson, G.D., Speers, G.C. (Eds.), Advances in Organic Geochemistry. Pergamon, pp. 55–67. https://doi.org/10.1016/B978-0-08-012758-3.50007-4.

Xiao, Q., McPherson, E.G., 2011. Rainfall interception of three trees in Oakland, California. Urban Ecosyst. 14 (4), 755–769. https://doi.org/10.1007/s11252-011-0192-5.

Xiao, Q., McPherson, E.G., Ustin, S.L., Grismer, M.E., 2000. A new approach to modeling tree rainfall interception. J. Geophys. Res. Atmos. 105 (D23), 29173–29188. https://doi.org/10.1029/2000JD900343.

Yao, L., Chen, L., Wei, W., Sun, R., 2015. Potential reduction in urban runoff by green spaces in Beijing: a scenario analysis. Urban For. Urban Green. 14 (2), 300–308. https://doi.org/10.1016/j.ufug.2015.02.014.